

 <p>ISSN NO. 2320-5407</p>	<p>Journal Homepage: - www.journalijar.com</p> <p>INTERNATIONAL JOURNAL OF ADVANCED RESEARCH (IJAR)</p> <p>Article DOI: 10.21474/IJAR01/11116 DOI URL: http://dx.doi.org/10.21474/IJAR01/11116</p>	
---	--	---

RESEARCH ARTICLE

COMPUTATIONAL APPROACH ON QUANTUM CHEMICAL ANALYSIS OF 2-BROMO-2-METHYL-1-PHENYLPROPAN-1-ONE

K. Rajalakshmi¹ and M. Vetrivel²

1. Assistant Professor, Department of Physics, SCSVMV, Kanchipuram.
2. Associate Professor, Department of Mechanical Engineering, SCSVMV, Kanchipuram.

Manuscript Info

Manuscript History

Received: 05 April 2020

Final Accepted: 07 May 2020

Published: June 2020

Key words:-

DFT, MESP, ELF, LOL, NBO, NLO

Abstract

The molecular geometry of 2-bromo-2-methyl-1-phenylpropan-1-one was optimized by DFT quantum chemical calculations and used to determine various molecular parameters theoretically. The HOMO and LUMO energy gap reveals that the energy gap reflects the chemical activity of the molecule. Global reactivity descriptors values are determined for the title molecule. Determination and visualization of molecule sites prone to electrophilic attack and nucleophilic attack performed by mapping of total density to the electron density surface is done by MESP Map analysis. Also, electron localization function (ELF) and localized orbital locator (LOL), determination of possible reactive centres of the title molecule realized by calculation of Fukui function analysis were carried out. Stability of the molecule arising from hyper conjugative interactions, charge delocalization has been analyzed using natural bond orbital (NBO) analysis. The possibility of being NLO active were studied by investigating the linear polarizability (α) and first-order hyperpolarizability (β) values computed using DFT quantum mechanical calculations. UV absorption spectra (in gas phase and in different solutions) were investigated by TD-DFT using B3LYP/6-311 +G(d,p) basis set and electronic properties such as excitation energies, oscillator strength and wavelength were tabulated.

Copy Right, IJAR, 2020,. All rights reserved.

Introduction:-

The reactivities of bromine-substituted (R-Br) or chlorine-substituted substrates (R-Cl) toward bromophilic or chlorophilic attack by a carbanion have been evaluated by intermolecular kinetics [1]. The reactions of this compound in which the bromine is on a tertiary carbon atom, with triethyl phosphite and with sodium diethyl phosphite take the same direction with formation of diethyl 2-methyl-1-propenyl phosphate [2]. Solvolysis involves treating the classified polymeric wastes with solvents and reagents to depolymerize the polymer to low molecular weight chemicals. A Grunwald-Winstein treatment of the specific rates of solvolysis of the compound in 100% methanol and in several aqueous ethanol, methanol, acetone, 2,2,2-trifluoroethanol (TFE), and 1,1,1,3,3,3-hexafluoro-2-propanol (HFIP) mixtures gives a good logarithmic correlation against a linear combination of N_T (solvent nucleophilicity) and Y_{Br} (solvent ionizing power) values. The pairing of DMSO and oxalyl bromide is reported as a highly efficient brominating reagent for various alkenes, alkynes and ketones. This bromination approach demonstrates remarkable advantages, such as mild conditions, low cost, short reaction times, provides

excellent yields in most cases and represents a very attractive alternative for the preparation of dibromides and α -bromoketones [3-4].

Computational details

The quantum chemical calculations of the title compound were performed with Gaussian 09 program package [5] employing Becke-Lee-Yang-Parr functional (B3LYP) [6-7]. The structure of the compound was optimized using Density functional theory (DFT) using 6-311 +G(d,p) basis set. The molecular structure, MEP surfaces were visualized with Gauss View 5 program [8]. The physico-chemical properties such as Frontier molecular orbitals, molecular electrostatic potential map (MEP), thermodynamic and non-linear optical structural parameters were calculated. The electronic absorption spectrum was calculated using the time-dependent density functional theory (TD-DFT) in water, DMSO and ethanol solution.

Results and Discussions:-

Molecular Geometry

The title compound has 23 atoms. A molecule consisting of N atoms has a total of 3N degrees of freedom, corresponding to the Cartesian coordinates of each atom in the molecule. In a nonlinear molecule, 3 of these degrees belong to the rotational, 3 of these degrees belong to the translational motions of the molecule and so the remaining corresponds to its vibrational motions. The net number of the vibrational modes is 3N-6. Therefore, for the title compound, three Cartesian displacements of 23 atoms provide 63 normal vibration modes. The molecular structure of the molecule with atom numbering is shown in Fig.1.

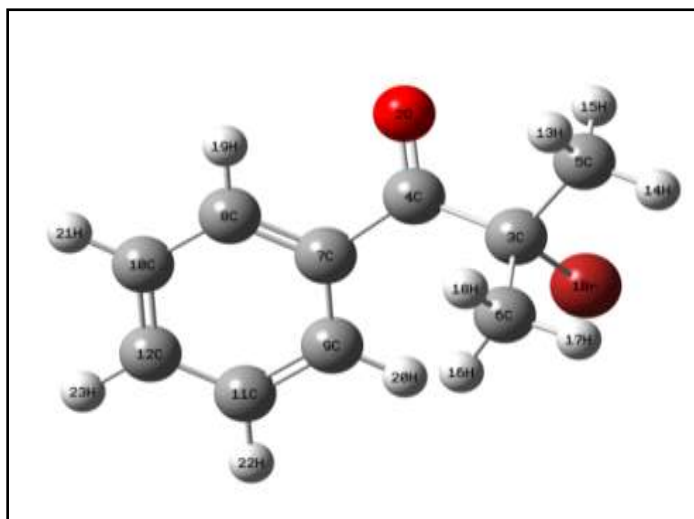


Fig.1:- Molecular structure of the title compound with atom numbering.

Topological analysis

Frontier molecular orbitals

The frontier molecular orbitals and their properties are important for predicting the most reactive position in π - electron system and several types of reactions in conjugated systems. [9-10]. The energy of the highest occupied molecular orbital (HOMO) is directly proportional to the ionization potential and characterizes the susceptibility of the molecule towards the attack of the electrophiles and the lowest unoccupied molecular orbital (LUMO) is related to the electron affinity and characterizes the susceptibility of the molecule towards the attack by nucleophiles [11]. The HOMO and LUMO values of the title compound are 7.254559 eV and 2.2705191eV respectively. The value of the energy gap is calculated to be 4.984040 eV which clearly indicates that charge transfer occur within the molecule and increasing the molecular activity. The HOMO-LUMO molecular orbitals are shown in Fig.2. It is clear from the HOMO-LUMO figure that HOMO is mainly situated over oxygen, bromine and ring atoms attached to oxygen atom while LUMO is mainly localized on atoms attached to oxygen and bromine atoms.

Global reactivity descriptors are presented in Table.1. The chemical reactivity descriptors of compounds such as electro negativity (χ), chemical potential (μ), hardness (η), softness (S) and electrophilicity index (ω) are evaluated using the following equations given below [12]:

$$\chi = \frac{I+A}{2}$$

$$\mu = -\frac{I-A}{2}$$

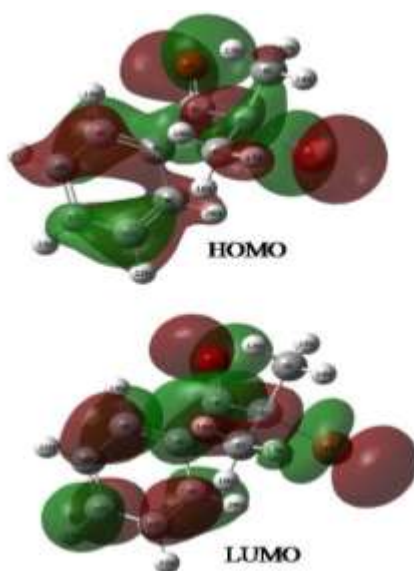
$$\eta = \frac{I-A}{2}$$

$$S = \frac{1}{2\eta}$$

$$\omega = \mu^2/2\eta$$

Table.1:- Calculated molecular parameters of the title compound.

Parameters	B3LYP/6-311+ G(d,p)
SCF energy (a.u.)	-3037.18807
Field Independent Dipole moment (Debye)	
μ_x	-2.2130
μ_y	1.1726
μ_z	3.2135
μ_{total}	4.0742
Zero point vibrational energy (kcal/mol)	115.40327
Total thermal energy (kcal/mol)	122.791
Molar heat capacity at const.volume C_v (cal mol ⁻¹ K ⁻¹)	44.313
Total entropy, S (cal mol ⁻¹ K ⁻¹)	108.478
Vibrational Energy (Kcal/Mol)	
Frontier Molecular Orbital Energies (eV)	
E_{HOMO} (eV)	7.254559
E_{LUMO} (eV)	2.270519
$E_{HOMO} - LUMO$ gap (eV)	4.984040
Global Reactivity Descriptors (eV)	
Chemical hardness (η)	2.49202
Softness (S)	0.20064
Chemical potential (μ)	4.76253
Electrophilicity index (ω)	4.55088

**Fig.2:-** Homo-Lumo Figure of the title compound.

Molecular electrostatic potential analysis

The molecular electrostatic potential (MEP) is related to electronic density and a very useful descriptor for determining the sites for nucleophilic and electrophilic reactions [13]. The different values of electrostatic potential are represented by different colours and the potential increases in the order of red<orange<yellow<green<blue. From this surface, we can interpret that the most residing areas of electron density (denoted by more red areas) and least electron density residing areas (denoted by deep blue areas). The color code of the map was found to be in the range $-4.417\text{e-}2$ (deepest red color has negative extreme) to $4.417\text{e-}2$ (deepest blue color has positive extreme). In the present MEP map, the maximum negative represents the site for electrophilic attack indicated by red colour while the maximum positive region represents the nucleophilic attack indicated by blue colour. The MEP map of the investigated compound (Fig.3 (a)) shows the regions of negative potential over the electronegative oxygen atom of the carbonyl group and less negative indicated by yellowish blob over the bromine atom and the regions having the positive potential are over the hydrogen atoms.

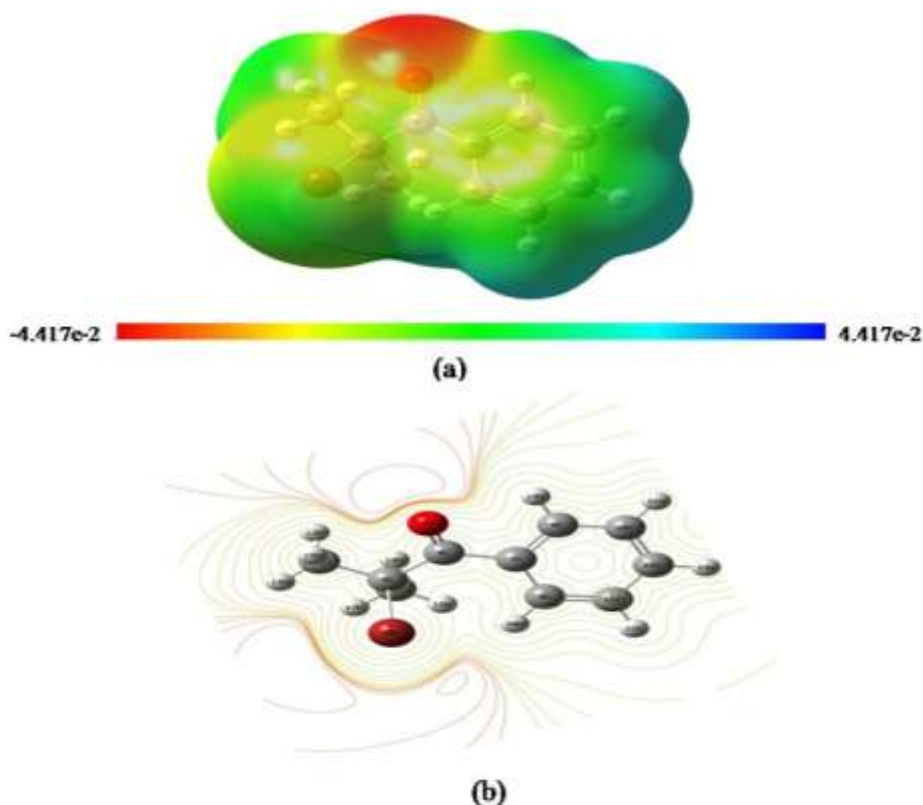


Fig.3 (a):- MEP map of the title compound. **(b) MEP Contour map of the title compound**

From Fig.3(b), it is clear that Br₁ and O₂ atoms are negatively charged as the local vdW surface are closer to bromine and have largely intersected solid contour lines around bromine and oxygen atoms. This can be further verified from the calculation for Hirshfeld atomic charges by Multiwfn program [14] for this molecule tabulated in Table.2.

Table.2:- Hirshfeld atomic charges of the title compound.

Element Name	Atomic charge
Br ₁	-0.06889
O ₂	-0.22011
C ₃	0.05310
C ₄	0.15272
C ₅	-0.09154
C ₆	-0.08723

C ₇	-0.01449
C ₈	-0.02459
C ₉	-0.03068
C ₁₀	-0.03449
C ₁₁	-0.03563
C ₁₂	-0.02557

Electron Localization function analysis

The modern method for investigating electronic structure of molecules free from arbitrary choice of molecular orbitals used in this study is the topological analysis of ELF as proposed by Silvi and Savin [15-16] belonging to quantum chemical topology [17]. The analysis such as ELF, LOL, Hole-Electron distribution Figures and Fukui Functions figures were performed using Multiwfn 3.7. [14] which is a multifunctional wave function analysis program. An electronic structure of a molecule described by ELF is represented by maxima (attractors) and its localization basin of $\eta(r)$ field, which characterize covalent bonds, lone pairs, core regions and valence shells in atoms. Calculated electron populations on chemical bonds, \bar{N} , is related to integration electron density over localization basins. results represent average values with quantum uncertainty. The topological analyses of the Electron Localization function (ELF) and Localized orbital locator (LOL) are tools used for performing covalent bonding analysis as they reveal regions of molecular space where the probability of finding an electron pair is high [18-19].

The topological analysis has been carried out for ELF for the title compound. The 2D map of ELF of the title compound shown in Fig.4 defined by atoms Br, O and H. It can be viewed that the covalent regions have high electron localization value (red region), the electron depletion regions between valence shell and inner shell are shown by the blue circles around nuclei. It is clear from the 2D map, that the chemical bonds C-O and C-Br are described by irregular localization domains (orange) with smaller values of electron localization (0.8-0.9) and these bonds have a covalent character and exhibit high electron localization of shared electron (covalent) bonding.

Also, high (≈ 1) values of electron localization is observed around hydrogen atoms indicating the presence of highly localized bonding and non-bonding electrons. The blue regions around few carbon atoms show the delocalized electron cloud around it.

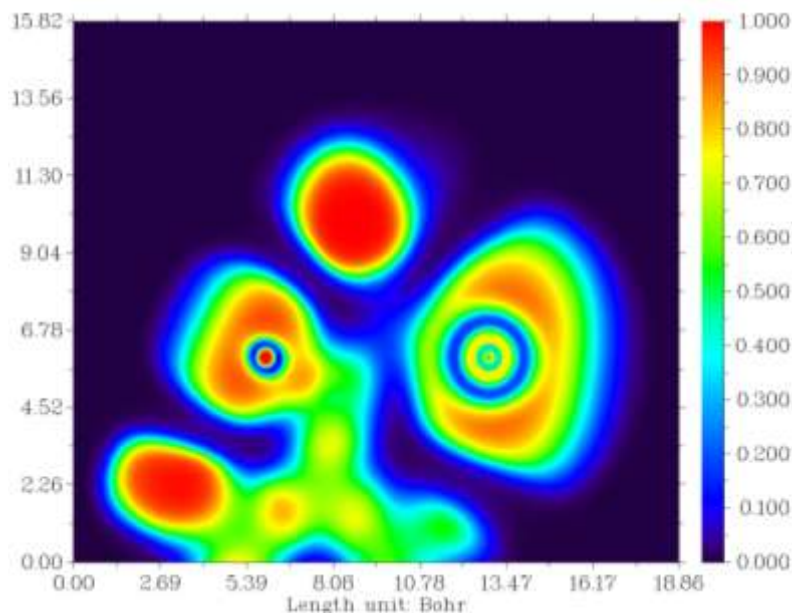


Fig 4:- The 2D map of ELF of the title compound defined by Br,O and H atoms.

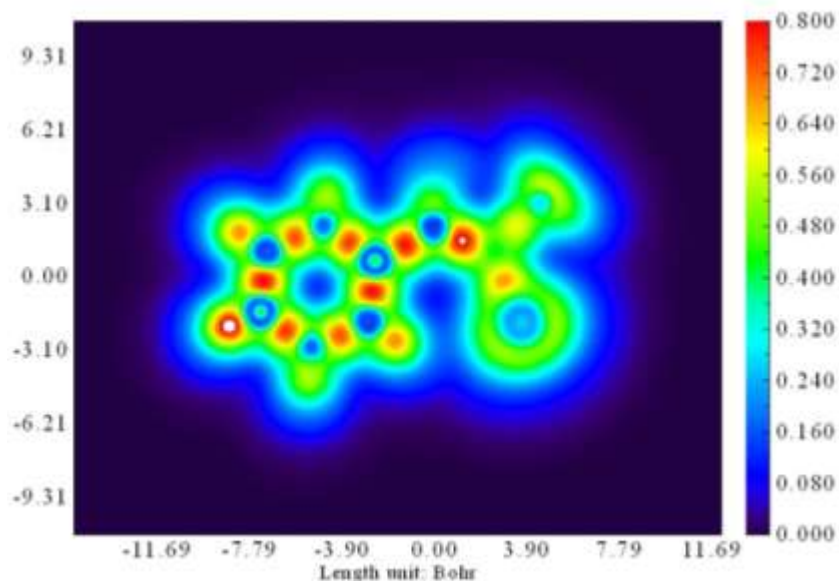


Fig.5:- LOL colour filled map of the title compound.

Localized orbital locator analysis

Molecular orbitals that are concentrated in a limited spatial region constitute the Localized molecular orbitals. Fig. 5 shows the LOL distribution under B3LYP/6-311 +G(d,p) method. It is clear that red colour intrudes into the interstitial space between the boundary atoms. From NBO analysis, a low stabilization energy is observed between Carbon-Bromine bonds and it is reflected as comparatively low values in LOL Figure and seen as distortion between Br1-C3 bond [20].

NBO analysis

Natural Bond Orbital (NBO) calculations were performed using NBO 3.1 program [21] as implemented in the Gaussian 09 package at DFT/B3LYP levels. The second order Fock-matrix was carried out to evaluate the donor (i) and acceptor (j) interaction in the NBO basis [22]. For each donor (i) and acceptor (j), the stabilization energy $E^{(2)}$ is associated as:

$$E^{(2)} = E_{ij} = q_i \frac{F(i,j)^2}{(\epsilon_i - \epsilon_j)}$$

The electron transfers from filled bonding orbital (donor) to empty antibonding orbitals (acceptor) [23-25] leading to hyperconjugative interactions can be examined by employing NBO analysis. The donor-acceptor interactions in NBO basis were evaluated using the second order Fock matrix. [26-27]. The larger the $E^{(2)}$ value, the more intensive is the interaction between electron donor and electron acceptor which means more donating tendency from electron donors to acceptors and a greater extent of conjugation of the whole system and the possible intensive interactions and the perturbation energies obtained by NBO analysis are listed in Table.3.

Table.3:- Second order perturbation theory analysis of Fock matrix in NBO basis of the title compound.

Donor (i)	Type	ED/e	Acceptor (j)	Type	ED/e	$E(2)^a$ (Kcal/mol)	$E(j) - E(i)^b$ (a.u)	$F(i,j)^c$ (a.u)
Br1-C3	σ	1.95584	O2-C4	σ^*	0.01049	0.85	1.15	0.028
O2-C4	π	1.99328	Br1-C3	σ^*	0.07559	3.41	0.41	0.034
O2-C4	σ	1.99328	C7-C9	σ^*	0.02390	1.36	1.65	0.042
C5-H14	σ	1.98506	C3-C4	σ^*	0.08309	3.91	0.84	0.052
C6-H16	σ	1.98576	C3-C5	σ^*	0.01904	3.53	0.89	0.050
C7-C9	π	1.63931	C7-C8	σ^*	0.02213	4.00	1.26	0.063
C7-C9	π	1.63931	O2-C4	π^*	0.12990	15.11	0.27	0.061
C7-C9	π	1.63931	C11-C12	π^*	0.32209	18.60	0.28	0.065
C8-C10	π	1.65080	C7-C9	π^*	0.36928	18.83	0.28	0.065

C8-C10	π	1.65080	C11-C12	π^*	0.32209	21.74	0.28	0.070
C8-H19	σ	1.97835	C7-C9	σ^*	0.02390	4.44	1.07	0.062
C9-H20	σ	1.97839	C7-C8	σ^*	0.02213	4.31	1.08	0.061
C10-H21	σ	1.97975	C7-C8	σ^*	0.02213	3.89	1.08	0.058
C11-C12	π	1.64569	C7-C9	π^*	0.36928	22.44	0.28	0.071
C11-C12	π	1.64569	C8-C10	π^*	0.29231	18.02	0.29	0.065
C11-C12	σ	1.97989	C9-C11	σ^*	0.01658	2.77	1.28	0.053
C11-C12	σ	1.97989	C10-C12	σ^*	0.32209	2.58	1.28	0.051
C11-H22	σ	1.97974	C7-C9	σ^*	0.02390	3.99	1.08	0.59
C11-H22	σ	1.97974	C10-C12	σ^*	0.32209	3.63	1.09	0.56
C12-H23	σ	1.98044	C9-C11	σ^*	0.01658	3.73	1.10	0.058
LP Br1	σ	1.99450	C3-C6	σ^*	0.02268	0.65	1.36	0.027
LP Br1	π	1.97593	C3-C6	σ^*	0.02268	1.74	0.66	0.030
LP O2	σ	1.97788	C4-C7	σ^*	0.06299	1.67	1.11	0.039
LP O2	π	1.88463	C3-C4	σ^*	0.08309	21.13	0.62	0.103
LP O2	π	1.88463	C4-C7	σ^*	0.06299	18.37	0.69	0.102

In the title molecule, π (C11-C12) \rightarrow π^* (C7-C9) and π (C11-C12) \rightarrow π^* (C8-C10), leading to stabilization energy of 22.44, 18.02(Kcal/mol), π (C8-C10) \rightarrow π^* (C11-C12) and π (C8-C10) \rightarrow π^* (C7-C9), leading to stabilization energy of 21.74, 18.83(Kcal/mol), π (C7-C9) \rightarrow π^* (C11-C12) and π (C7-C9) \rightarrow π^* (O2-C4) has 18.60 and 15.11 (Kcal/mol) respectively and hence they give stronger stabilization to the structure. The stabilization of some of the ring is due to the interaction between C-C to anti bond of C-C in the ring as evident from the Table. 3.

Also interaction between LP(2) O2 \rightarrow σ^* (C3-C4) and LP(2) O2 \rightarrow σ^* (C4-C7) leads to stabilization of 21.13 and 18.37kcal/mol. All these transitions with stabilization energies correspond to only three pairs of orbitals (C7-C9),(C8-C10) and (C11-C12) taking place in both forward and reverse direction among the orbitals within the ring structure.

Condensed Fukui Function

The Fukui function describes the electron density after adding or removing some amount of electrons. R.G.Parr and W.Yang [28] reported condensed Fukui function and frontier function. The local reactivity descriptor like Fukui function indicates the preferred regions where a molecule will alter its density or indicates its natural tendency to deform at a given position on accepting or donating electron HUMO or LUMO [29]. The theoretical tool Fukui function was performed by UCA-FUKUI software to understand the chemical reactivity, the condensed Fukui function and related local and global parameters were calculated [30]. In order to find the chemical reactivity and selectivity of the specific atomic site in a molecule, condensed Fukui function and local softness are used [30-31]. The Fukui functions at the atom k result to be:

$$f_k^\alpha = \sum_{v=k} \left[|C_{v\alpha}|^2 + \sum_{x \neq \mu} C_{x\alpha}^* C_{v\alpha} S_{xv} \right]$$

where $C_{v\alpha}$ are the molecular frontier orbitals coefficients and S_{xv} are the atomic orbital overlap matrix elements

$$f_k^- = \sum_{v \neq k} \left[|C_{vH}|^2 + \sum_{x \neq \mu} C_{xH}^* C_{vH} S_{xv} \right] \text{ [for HOMO electrophilic attack]}$$

$$f_k^+ = \sum_{v \neq k} \left[|C_{vL}|^2 + \sum_{x \neq \mu} C_{xL}^* C_{vL} S_{xv} \right] \text{ [for LUMO Nucleophilic attack]}$$

$$f_k^0 = \frac{1}{2} (f_k^+ + f_k^-) \text{ [for radical attack]}$$

The sub-indexes "H" and "L" refers to HOMO and LUMO orbitals. When a molecule gains electrons, it has the reactivity site of electrophilic attack f_k^- , when the molecule losses electrons, it has reactivity site for nucleophilic attack f_k^+ , and when the molecule has neutral electrons, they are in radical attack. Local electrophilicity, Local Nucleophilicity, Hardness and second order Fukui functions are called Dual-Descriptor Δf_r and by using finite difference approximation [31-33], it can be defined as:

$$\begin{aligned} W_k^+ &= W f_k^+ && \text{For local Electrophilicity} \\ W_k^- &= W f_k^- && \text{For local Nucleophilicity} \\ \eta_k &= \epsilon_L f_k^+ - \epsilon_H f_k^- && \text{For local Hardness} \\ \Delta f_r &= |(f_r^+ - f_r^-)| && \text{For dual descriptor} \end{aligned}$$

Table.4:- Condensed Fukui Functions evaluated by Frontier Molecular Orbital method for the title compound.

Atom	Atomic Number	HOMO Electrophilic attack (f_k^-)	LUMO Nucleophilic attack (f_k^+)	Radical Attack (f_k^0)	Dual-Descriptor (Δf_r)	Hardness (au)	Local Electrophilic W-(eV)	Local Nucleophilic W (eV)
Br ₁	35	0.0000	0.0028	0.0014	0.0028	0.0000	0.0000	0.0024
O ₂	8	0.0002	0.2165	0.1083	0.2163	0.0009	0.0001	0.1849
C ₃	6	0.0007	0.0628	0.0318	0.0621	0.0004	0.0006	0.0536
C ₄	6	0.0108	0.5997	0.3052	0.5889	0.0053	0.0092	0.5120
C ₅	6	0.0001	0.0006	0.0003	0.0004	0.0000	0.0001	0.0005
C ₆	6	0.0003	0.0141	0.0072	0.0138	0.0001	0.0002	0.0120
C ₇	6	0.1164	0.0386	0.0775	-0.0778	0.0308	0.0994	0.0329
C ₈	6	0.4912	0.0300	0.2606	-0.4612	0.1293	0.4194	0.0256
C ₉	6	0.0507	0.0102	0.0305	-0.0405	0.0134	0.0433	0.0087
C ₁₀	6	0.2899	0.0213	0.1556	-0.2686	0.0763	0.2475	0.0181
C ₁₁	6	0.0218	0.0002	0.0110	-0.0216	0.0057	0.0186	0.0002
C ₁₂	6	0.0179	0.0016	0.0097	-0.0163	0.0047	0.0152	0.0013

The condensed Fukui functions using FMO theory were calculated and listed in Table.4. It is observed that maximum electrophilic attack order are $C_8 > C_{10} > C_7 > C_9 > C_{11} > C_{12} > C_4 > C_3 > C_6 > O_2 > C_5$ and the maximum nucleophilic attack order are $C_4 > O_2 > C_3 > C_7 > C_8 > C_{10} > C_6 > C_9 > Br_1 > C_{12} > C_{11}$. The highest radical attack order was found to be $C_4 > C_8 > C_{10} > O_2 > C_7 > C_9$ atoms [34].

The Fukui function of the system defines the most reactive regions in a molecule. The individual atomic charges deliberated by Frontier Molecular Orbital and Natural Population analysis (NPA) have been used to calculate the Condensed Fukui function (CFF). Kolandaivel et al. [35] introduced the atomic descriptor to determine the local reactive sites of the molecular structure. The reactivity indices are directly concerned with the selectivity of the molecule. Using the NPA charges of neutral (radical), negative (cation) and positive (anion) state of a present molecule, Fukui function $f^+(\vec{r})$, $f^-(\vec{r})$, $f^0(\vec{r})$ are calculated. Fukui function are calculated using the following solutions:

$$f^+(\vec{r}) = q_r(N+1) - q_r(N) \text{ for nucleophilic attack}$$

$$f^-(\vec{r}) = q_r(N) - q_r(N-1) \text{ for electrophilic attack}$$

$$f^0(\vec{r}) = q_r(N+1) - q_r(N-1) \text{ for radical attack}$$

where +, - and 0 show the nucleophilic, electrophilic and radical attack respectively.

Table.5:- Condensed Fukui function (f_k^+ , f_k^- , f_k^0) and dual-descriptor (Δf_k) evaluated by Natural Population Analysis

Atoms	Natural Population analysis			Condensed Fukui function			Dual-descriptor
(N)	Cation	Anion	Neutral	f_k^-	f_k^+	f_k^0	(Δf_k)
Br ₁	0.18920	-0.24334	0.01971	0.16949	0.26305	0.43254	0.09356
O ₂	-0.28659	-0.68746	-0.51678	0.23019	0.17068	0.40087	-0.05951
C ₃	-0.18188	-0.21403	-0.16784	-0.01404	0.04619	0.03215	0.06023
C ₄	0.59091	0.36036	0.56437	0.02654	0.20401	0.23055	0.17747
C ₅	-0.59425	-0.58409	-0.58862	-0.00563	-0.00453	0.01016	0.0011
C ₆	-0.61119	-0.59353	-0.59799	-0.0132	-0.00446	0.01766	0.00874
C ₇	-0.04334	-0.06964	-0.13138	0.08804	-0.06174	0.0263	-0.14978
C ₈	-0.16084	-0.20154	-0.19211	0.03127	0.00943	0.0407	-0.02184
C ₉	-0.15976	-0.22422	-0.18968	0.02992	0.03454	0.06446	0.00462
C ₁₀	-0.15880	-0.23953	-0.18893	0.03013	0.0506	0.08073	0.02047

C ₁₁	-0.15729	-0.21753	-0.18714	0.02985	0.03039	0.06024	0.00054
C ₁₂	-0.06403	-0.24647	-0.20545	0.14142	0.04102	0.18244	-0.1004

The condensed Fukui function (f_k^+ , f_k^- , f_k^0) and Dual-descriptor (Δf_k) evaluated by NPA listed in Table.5. It is found that dual descriptor (Δf_k) value is highly positive for Br₁ having tendency to acquire electron and C₅ is electrophilic [36] and Condensed Fukui function figures (f_k^- , f_k^0 , Δf_k) for the title compound is presented in Fig.6.

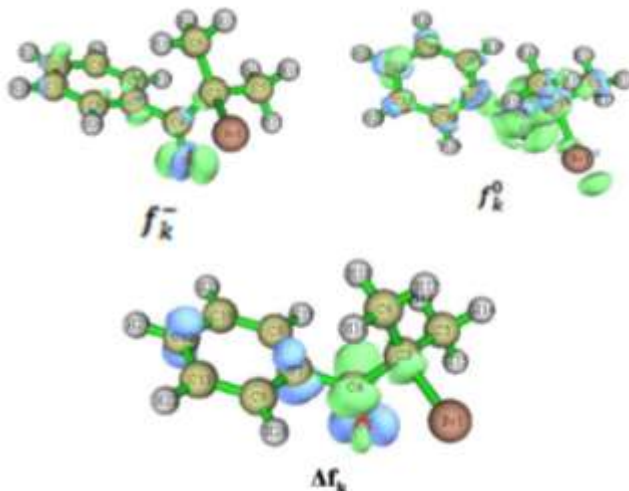


Fig.6:- Condensed Fukui function (f_k^- , f_k^0 , Δf_k) for the title compound.

Nonlinear optical (NLO) property analysis

The first order hyperpolarizability (β), polarizability (α) and dipole moment (μ) were calculated using B3LYP/6-311+G(d,p) level of the finite field approach. The complete equations for calculating the magnitude of total static dipole moment, polarizability and first-order polarizability using the x,y,z components from Gaussian '09 output are as follows:

$$\mu_{\text{tot}} = (\mu_x^2 + \mu_y^2 + \mu_z^2)^{1/2}$$

$$\alpha_{\text{tot}} = \frac{1}{3} (\alpha_{xx} + \alpha_{yy} + \alpha_{zz})$$

$$\beta_{\text{tot}} = [(\beta_{xxx} + \beta_{xyy} + \beta_{xzz})^2 + (\beta_{yyy} + \beta_{yzz} + \beta_{yxx})^2 + (\beta_{zzz} + \beta_{zxx} + \beta_{zyy})^2]^{1/2}$$

The calculated values of dipole moment, polarizability and hyper-polarizability are given in Table.6. The calculated dipole moment is 3.0516 Debye, polarizability α_{tot} is equal to 5.265370×10^{-24} e.s.u and have non-zero values and was dominated by diagonal components. The first-order polarizability is found to be 2.9002×10^{-30} e.s.u which is nearly 5 times that of urea [37]. Our title compound with greater dipole moment and hyperpolarizability value shows that the compound has large NLO optical property.

Table.6:- Dipole moment, Polarizability and hyperpolarizability of the title compound.

Dipole moment		Polarizability		Hyperpolarizability	
Components	Value (Debye)	Components	Value (a.u.)	Components	Value (a.u.)
μ_x	-1.5142	α_{xx}	176.112871	β_{xxx}	-345.489136
μ_y	-0.6562	α_{yy}	-0.015847	β_{xyy}	54.78063
μ_z	2.5669	α_{zz}	143.662352	β_{xyy}	25.061213
μ_{tot} (D)	3.0516	α_{xy}	2.009714	β_{yyy}	101.433255
		α_{xz}	5.038148	β_{xxz}	32.716809
		α_{yz}	102.628238	β_{xyz}	-3.696230

		$\alpha_{\text{tot}} \times 10^{-24}$ (esu)	5.265370×10^{-24}	β_{yyz}	-10.699195
				β_{xzz}	4.603320
				β_{yzz}	-46.09655
				β_{zzz}	6.676574
				β_{tot} (esu)	2.9002×10^{-30}
				β_{tot} (compound) / β_{tot} urea	4.779

Theoretically, the first hyperpolarizability of the title compound is 4.779 times magnitude of urea. Domination of particular component indicates on a substantial delocalization of charges in that direction. In the present study, the biggest value of hyperpolarizability is noticed in β_{yyz} direction and subsequently delocalization of electron cloud is more in that direction. The maximum β value may be due to π -electron cloud movement from donor to acceptor which makes the molecule highly polarized and intramolecular charge transfer possible. So, from the magnitude of first hyperpolarizability, the title compound may be a potential applicant in the development of NLO materials.

Electronic excitation analysis

The electronic excitation analysis of the title compound has been carried out using TD-DFT method using B3LYP/6-311 +G(d,p) basis sets. The comparative theoretical UV absorption spectra in gas phase and in three solvents ethanol, water and DMSO is presented in Fig.7. Due to specific solute-solute and solute-solvent interaction in form of hydrogen bonding, the intensities, positions and shapes of the electronic absorption bands are usually altered when the absorption spectra are recorded in solvents of different polarity. The calculated results involving vertical excitation energies, oscillator strengths (f) and wavelength are tabulated in Table.7. According to Frank-Condon principle, the maximum absorption (λ_{max}) correspond to vertical excitation in UV spectrum [38]. It is observed the very intense electronic transition occur at 333.87, 333.69, 333.52 with oscillator strength 0.0028, 0.0029 and 0.0028 for Ethanol, DMSO and water. Moreover, the theoretical wavelength in gas phase is found to be higher i.e. 339.92 nm than the wavelength in different solvents.

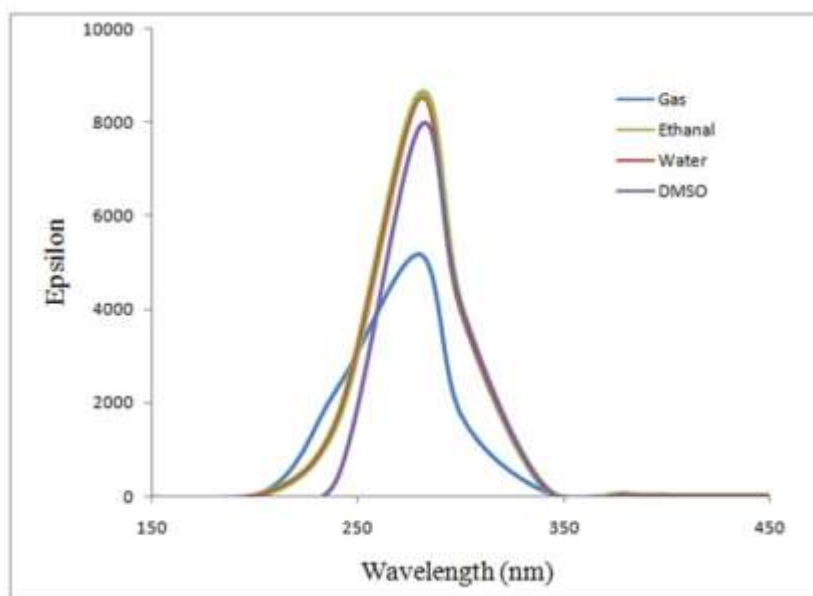


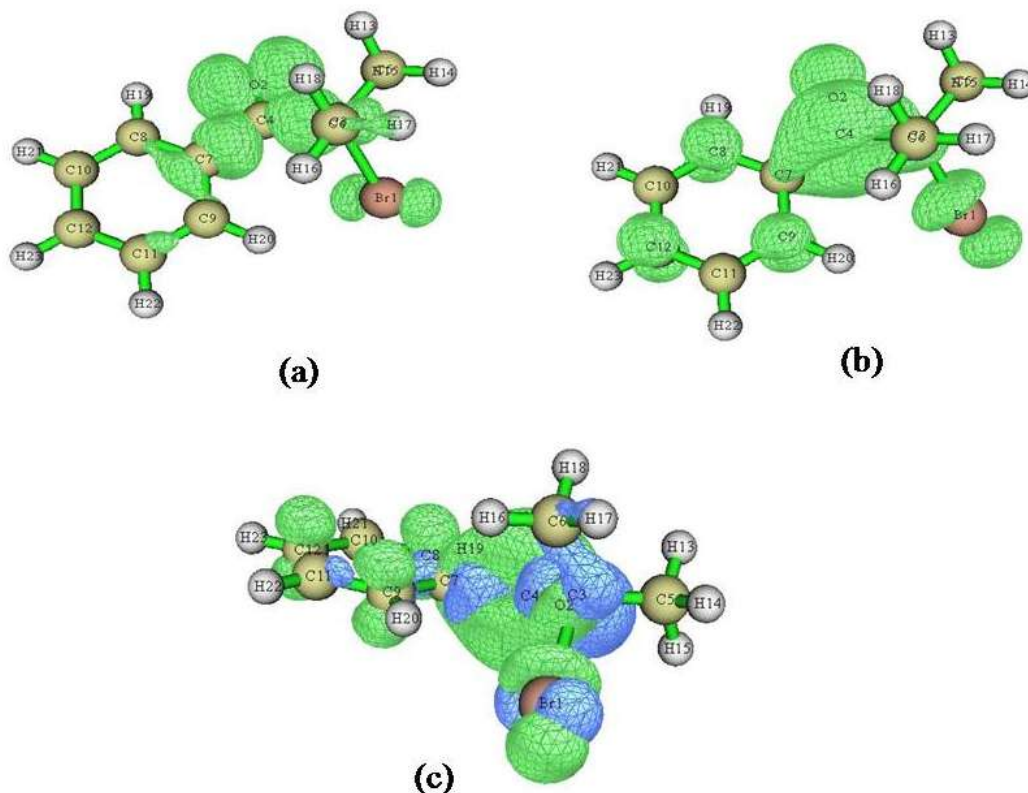
Fig.7:- Comparative Theoretical UV-Visible spectrum of the title compound.

The calculated band at 339.92 nm in theoretical spectrum corresponds to transition from HOMO-6 to LUMO (13.69%). The second dominant band observed at 278.73 corresponds to transition from HOMO-4 to LUMO (24.37%) while the third dominant band at 272.72 corresponds to the transition from HOMO to LUMO (79.68%).

Table.7:- Electronic Energy, Wavelengths and Oscillator strengths calculated at TD-DFT method for the title compound.

Solvent	Excited state	Band Gap (eV)	Energy (cm ⁻¹)	Wavelength λ (nm)	Oscillator strength
Gas phase	S ₁	3.6475	29,419	339.92	0.0023
	S ₂	4.4482	35,877	278.73	0.0118
	S ₃	4.5461	36,666	272.73	0.0831
DMSO	S ₁	3.7155	29,967	333.69	0.0029
	S ₂	4.3348	34,962	286.02	0.0177
	S ₃	4.4768	36,107	276.95	0.1809
Ethanol	S ₁	3.7135	29,951	333.87	0.0028
	S ₂	4.3393	34,998	285.73	0.0170
	S ₃	4.4821	36,150	276.62	0.1739
Water	S ₁	3.7175	29,983	333.52	0.0028
	S ₂	4.3352	34,965	285.99	0.0167
	S ₃	4.4817	36,147	276.64	0.1724

The distribution of hole, electron and both simultaneously are shown in Fig.8. It can be observed that there is a spatial separation between the hole-electron distribution thus indicating the charge transfer.

**Fig.8:- Visualization of (a) Hole distribution (b) Electron distribution (c) Hole-Electron distribution**

Conclusion:-

The optimization of structure geometry was done at DFT/B3LYP/6-311 +G(d,p) functional for analysis various molecular properties of the title compound. The significant difference in HOMO-LUMO energy gap supports the charge transfer within the molecule. The MEP map of the investigated compound shows the regions of negative potential over the electronegative oxygen atom of the carbonyl and the regions having the positive potential are over the hydrogen atoms. The chemical bonds C-O and C-Br are described by irregular localization domains with smaller

values of electron localization is observed from 2D map of ELF. It is clear from NBO analysis that most of transitions with stabilization energies correspond to only three pairs of orbitals (C7-C9),(C8-C10) and (C11-C12) and interaction between LP(2) O2 \rightarrow σ^* (C3-C4) and LP(2) O2 \rightarrow σ^* (C4-C7) leads to stabilization of 21.13 and 18.37kcal/mol. The sites of electrophilic and nucleophilic were determined using Fukui functions. UV absorption spectra (in gas phase and in different solutions) were investigated by TD-DFT using B3LYP/6-311 +G(d,p) basis set and electronic properties such as excitation energies, oscillator strength and wavelength were tabulated. NLO calculations showed that the first hyperpolarizability of the title compound is 4.779 times magnitude of urea suggesting that the title compound is NLO active.

References:-

1. Fu W., Zhang X. Jiang X. (2001). Relative reactivities of halogen-substituted substrates (R-Br, R-Cl) toward the halophilic attack by a carbanion. Sc. China Ser. B-Chem. 44, 337-343.
2. Arbuzov, B.A., Vinogradova, V.S., Polezhaeva, N.A. et al. (1963). β -Keto phosphonic esters Communication 12. Structures of the products of the reaction of some α -halo ketones of the aromatic series with triethyl phosphite and with sodium diethyl phosphite. Russ Chem Bull, 12, 1257-1264.
3. Rui Ding, Jiaqi Li, Wenyi Jiao, Mengru Han, Yongguo Liu, Hongyu Tian, Baoguo Sun, (2018). A Highly Efficient Method for the Bromination of Alkenes, Alkynes and Ketones Using Dimethyl Sulfoxide and Oxalyl Bromide, Synthesis; 50(21): 4325-4335.
4. Dennis Neil Kevill, Chang-Bae Kim, Malcolm John D'Souza, (2018). Correlation of the Rates of Solvolysis of α -Bromoisobutyrophenone Using Both Simple and Extended Forms of the Grunwald-Winstein Equation and the Application of Correlation Analysis to Related Studies, Eur J Chem, 9(1):1-6.
5. Frisch MJ., et al., Gaussian 09, Revision B.01, Gaussian Inc., Wallingford CT2009.
6. Becke AD., (1993). Density-functional thermochemistry., III. The role of exact exchange. The Journal of Chemical Physics; 98(7),5648-5652.
7. Lee C., Yang W., Parr RG., (1988). Development of the Colle- Salvetti correlation energy formula into a functional of the electron density. Physical Review B, 37 (2) 785-789.
8. Frisch E., Hratchian HP., Dennington II RD., Keith TA., Millam J., Nielsen B., Holder AJ., Hiscocks J., (2009).Gaussian, Inc. GaussView Version 5.0.8, Wallinford, CT.
9. Sheena Y.,Mary., Ebtehal S., Al.Abdullah., Haya I Aljohar., Badiaka Narayana., Prakash S Nayak., Baladka K Sarojini., Stevan Armakovic., Sanja J.Armakovic., Christian Van Alsonoy., Ali A.El-Eman., (2018).4-[4-Acetylphenyl]amino]-2-methylidene-4-oxobutanoic acid, a newly synthesis amide with hydrophilic and hydrophobic segments:Spectroscopic characterization and investigation of its reactive properties, J.Serb.Chem.Soc.,83 (1),1-18.
10. Fukui K., Yonezawa T., Shingu H., (1952). A Molecular Orbital Theory of Reactivity in Aromatic Hydrocarbons,J.Chem.Phys. 20(4), 722-725.
11. Bhawani Datt Joshi, Poonam Tandon,Sudha Jain, (2013).Structure, MESP and HOMO-LUMO study of 10-Acetyl-10H-phenothiazine 5-oxide using vibrational spectroscopy and quantum chemical methods, BIBICHANA, 9, ,38-49.
12. Parr.R.J., Pearson R.G., (1983).Absolute hardness : comparison parameter to absolute electronegativity,J.Am.Chem.Soc.,105(26), 7512 -7516.
13. Kezeshury G.,Holly S., Besenyei G., Varga J.,Wang A.W.,Durig J.R., (1993). Spectrochim Acta, A 49 (13-14),2007-2017.
14. Tian Lu.,Feiwu Chen., (2012). Multiwfn: A Multifunctional Wavefunction Analyzer, J.Comput.Chem., 33,580-592.
15. Michal Michalski., Agnieszka J.Gordon., Slawomir Berski., (2019).Topological analysis of the electron localization function (ELF) applied to the electronic structure of oxaziridine: the nature of N-O bond, Structural Chemistry, 30, 2181-2189.
16. Silvi B.,Savin A., (1994).Classification of chemical bonds based on topological analysis of electron localization functions, Nature, 371, 683-686.
17. Malcolm N.,Popelier PLA.,(2003).The full topology of the Laplacian of the electron density-scrutinizing a physical basis for the VSEPR model, Faraday Discuss, 124, 353-363.
18. Fuentealba P.,Chamorro E., Santos JC., (2007).57 Chapter 5: Understanding and using the electron localization function, Theorec.Comp.Chem.,19, 57-85.
19. Jacobsen H.,(2009).Localized-orbital locator (LOL) profiles of transition-metal hydride and dihydrogen complexes, Can.J.Chem. 87, 695-973.

20. Christina Susan Abraham., Muthu S., Johanan Christian Prasanna., Stevan Armakovic, Sanja J., Armakovic, Fathima Rizwana B., Ben Geoffrey., Host Antony David R., (2019). Computational evaluation of the reactivity and pharmaceutical potential of an organic amine : A DFT, molecular dynamics simulations and molecular docking approach, *Spectrochimica Acta:Part A*, 222 ,117188.
21. Glendening ED., Reed AE., Carpenter JE., Weinhold F., (1998). NBO Version 3.1, TCI, University of Wisconsin, Madison.
22. Foster JP., Weinhold F., (1980). Natural hybrid orbitals. *Journal of the American Chemical Society*, 102(24), 7211-7218.
23. Reed A.E., Weinhold F., (1983). *J.Chem.Phys.* 78, 4066.
24. Ivanciuc O., Balaban A.T., Schleyer P., Allinger T., Clark J., Gasteiger J., Kollman P.A., Schaefer F., Schreiner P.R., (1998). *Encyclopedia of Computational Chemistry*, John Wiley & Sons, Chichester, 1169-1190.
25. Weinhold F., Landis C.R., (2005). *Valency and Bonding: A Natural Bond orbital Donor-Acceptor Perspective*, Cambridge University Press, Cambridge.
26. Reed A.E., Curtis LA, Weinhold F.A., (1988). Intermolecular interactions from a natural bond orbital, donor-acceptor viewpoint, *Chem.Rev.* 88(6), 899-926.
27. Chocholousova J, Vladimir Spirko V, Hobza P, (2004). First local minimum of the formic acid dimer exhibits simultaneously red shifted O-H...O and improper blue shifted C-H...O hydrogen bonds, *Phys.Chem.Chem.Phys.* 6, 37-41.
28. Parr R.G., Yang W., (1984). DFT approach to the frontier-electron theory of chemical reactivity, *J.Am.Soc.*, 106, 4049-4050.
29. Parr R.G., Szentpaly L.V., Liu S., (1999). Electrophilicity index, *J.Am.Soc.*, 121(9), 1922-1924.
30. Sanchez-Marquez., Zorrilla D., (2014). Introducing "UCA-FUKUI" software, reactivity-index calculations, *J.Mol.Model*, 20:2492.
31. Allison, T.C., Tong Y.G., (2013). Application of the Condensed Fukui function to predict reactivity in core-shell transition metal nanoparticles, *Ele.Chi.Acta.*, 101, 334-340.
32. Fuentealba P., Perez P., Contreras R., (2005). On the Condensed Fukui function, (2000). *J.Chem.Phys.* 113, 2544-2551.
33. Morell C., Grand A., Toro-Labbe A., (2005). New Dual Descriptor for Chemical Reactivity, *J.Phys.Chem.A*, 109 (1), 205-212.
34. Ramesh P., Lydia caroline M., Muthu S., Narayana B., Raja M., Ben Geoffrey A.S., (2019). Spectroscopic, chemical reactivity, molecular docking investigation and QSAR analyses of (2E) 1 (3 bromo 2 thienyl) 3 (2,5 dimethoxyphenyl) prop 2 en 1 one, *Spectrochimica Acta:Part A*, 222, 117190.
35. Kolandaivel P., Praveen G., (2005) Study of atomic and condensed atomic indices for reactive sites of molecules, *J.Chem.Sci.* 117, 591-598.
36. Anju L.S., Aruldas D., Hubert Joe I., Balachandran S., (2020). Density functional theory, spectroscopic and hydrogen bonding analysis of fenoxycarb-water complexes, 1201, 127201.
37. Sheela GE., Manimaran D., Hubert Joe I., Sherifa Rahim., Bena Jothy V., (2015). Structure and nonlinear optical property analysis of L-Methioninium oxalate: a DFT approach, *Spectrochim Acta*, 143, 40-48.
38. Benallal B., Boughrai H., Sahdane T., Essassi E.M., Kabouchi B., (2017). Theoretical and experimental investigations of structural and electronic properties of 1-Benzyl-3-methyl-quinoxalin-2(1H) one molecule, *J.Mater.Environ.Sci.* 8, 4657-4662.